

## Study of $\chi_{bJ}(2P) \rightarrow \omega\Upsilon(1S)$ at Belle

Z. S. Stottler<sup>1</sup>, T. K. Pedlar<sup>2</sup>, B. G. Fulsom<sup>3</sup>, I. Adachi<sup>4</sup>, K. Adamczyk<sup>5</sup>, H. Aihara<sup>6</sup>, S. Al Said<sup>7</sup>, D. M. Asner<sup>8</sup>, H. Atmacan<sup>9</sup>, T. Aushev<sup>10</sup>, R. Ayad<sup>11</sup>, V. Babu<sup>12</sup>, Sw. Banerjee<sup>13</sup>, M. Bauer<sup>14</sup>, P. Behera<sup>15</sup>, K. Belous<sup>16</sup>, J. Bennett<sup>17</sup>, F. Bernlochner<sup>18</sup>, M. Bessner<sup>19</sup>, T. Bilka<sup>20</sup>, D. Biswas<sup>21</sup>, A. Bobrov<sup>22</sup>, D. Bodrov<sup>23</sup>, G. Bonvicini<sup>24</sup>, J. Borah<sup>25</sup>, A. Bozek<sup>26</sup>, M. Bračko<sup>27</sup>, P. Branchini<sup>28</sup>, T. E. Browder<sup>29</sup>, A. Budano<sup>30</sup>, M. Campajola<sup>31</sup>, L. Cao<sup>32</sup>, D. Červenkov<sup>33</sup>, M.-C. Chang<sup>34</sup>, B. G. Cheon<sup>35</sup>, K. Chilikin<sup>36</sup>, H. E. Cho<sup>37</sup>, K. Cho<sup>38</sup>, S.-K. Choi<sup>39</sup>, Y. Choi<sup>40</sup>, S. Choudhury<sup>41</sup>, D. Cinabro<sup>42</sup>, S. Das<sup>43</sup>, G. De Nardo<sup>44</sup>, G. De Pietro<sup>45</sup>, R. Dhamija<sup>46</sup>, F. Di Capua<sup>47</sup>, Z. Doležal<sup>48</sup>, T. V. Dong<sup>49</sup>, S. Dubey<sup>50</sup>, P. Ecker<sup>51</sup>, D. Epifanov<sup>52</sup>, T. Ferber<sup>53</sup>, D. Ferlewicz<sup>54</sup>, V. Gaur<sup>55</sup>, A. Garmash<sup>56</sup>, A. Giri<sup>57</sup>, P. Goldenzweig<sup>58</sup>, E. Graziani<sup>59</sup>, T. Gu<sup>60</sup>, Y. Guan<sup>61</sup>, K. Gudkova<sup>62</sup>, C. Hadjivasiliou<sup>63</sup>, T. Hara<sup>64</sup>, K. Hayasaka<sup>65</sup>, S. Hazra<sup>66</sup>, M. T. Hedges<sup>67</sup>, D. Herrmann<sup>68</sup>, W.-S. Hou<sup>69</sup>, C.-L. Hsu<sup>70</sup>, K. Inami<sup>71</sup>, N. Ipsita<sup>72</sup>, A. Ishikawa<sup>73</sup>, R. Itoh<sup>74</sup>, M. Iwasaki<sup>75</sup>, Y. Iwasaki<sup>76</sup>, W. W. Jacobs<sup>77</sup>, S. Jia<sup>78</sup>, Y. Jin<sup>79</sup>, A. B. Kaliyar<sup>80</sup>, T. Kawasaki<sup>81</sup>, C. Kiesling<sup>82</sup>, C. H. Kim<sup>83</sup>, D. Y. Kim<sup>84</sup>, K.-H. Kim<sup>85</sup>, Y.-K. Kim<sup>86</sup>, P. Kodyš<sup>87</sup>, A. Korobov<sup>88</sup>, S. Korpar<sup>89</sup>, E. Kovalenko<sup>90</sup>, P. Križan<sup>91</sup>, P. Krokovny<sup>92</sup>, T. Kuhr<sup>93</sup>, M. Kumar<sup>94</sup>, R. Kumar<sup>95</sup>, K. Kumara<sup>96</sup>, A. Kuzmin<sup>97</sup>, Y.-J. Kwon<sup>98</sup>, Y.-T. Lai<sup>99</sup>, T. Lam<sup>100</sup>, M. Laurenza<sup>101</sup>, S. C. Lee<sup>102</sup>, D. Levit<sup>103</sup>, P. Lewis<sup>104</sup>, L. K. Li<sup>105</sup>, J. Libby<sup>106</sup>, K. Lieret<sup>107</sup>, D. Liventsev<sup>108</sup>, T. Luo<sup>109</sup>, Y. Ma<sup>110</sup>, M. Masuda<sup>111</sup>, S. K. Maurya<sup>112</sup>, F. Meier<sup>113</sup>, M. Merola<sup>114</sup>, K. Miyabayashi<sup>115</sup>, G. B. Mohanty<sup>116</sup>, R. Mussa<sup>117</sup>, I. Nakamura<sup>118</sup>, M. Nakao<sup>119</sup>, A. Natochii<sup>120</sup>, L. Nayak<sup>121</sup>, N. K. Nisar<sup>122</sup>, S. Nishida<sup>123</sup>, K. Ogawa<sup>124</sup>, S. Ogawa<sup>125</sup>, H. Ono<sup>126</sup>, P. Oskin<sup>127</sup>, P. Pakhlov<sup>128</sup>, G. Pakhlova<sup>129</sup>, T. Pang<sup>130</sup>, S. Pardi<sup>131</sup>, J. Park<sup>132</sup>, S.-H. Park<sup>133</sup>, S. Patra<sup>134</sup>, S. Paul<sup>135</sup>, R. Pestotnik<sup>136</sup>, L. E. Pilonen<sup>137</sup>, T. Podobnik<sup>138</sup>, E. Prencipe<sup>139</sup>, M. T. Prim<sup>140</sup>, N. Rout<sup>141</sup>, G. Russo<sup>142</sup>, Y. Sakai<sup>143</sup>, S. Sandilya<sup>144</sup>, A. Sangal<sup>145</sup>, L. Santelj<sup>146</sup>, V. Savinov<sup>147</sup>, G. Schnell<sup>148</sup>, C. Schwanda<sup>149</sup>, Y. Seino<sup>150</sup>, K. Senyo<sup>151</sup>, W. Shan<sup>152</sup>, M. Shapkin<sup>153</sup>, C. Sharma<sup>154</sup>, J.-G. Shiu<sup>155</sup>, A. Sokolov<sup>156</sup>, E. Solovieva<sup>157</sup>, M. Starič<sup>158</sup>, M. Sumihama<sup>159</sup>, W. Sutcliffe<sup>160</sup>, M. Takizawa<sup>161</sup>, U. Tamponi<sup>162</sup>, K. Tanida<sup>163</sup>, F. Tenchini<sup>164</sup>, R. Tiwary<sup>165</sup>, M. Uchida<sup>166</sup>, Y. Unno<sup>167</sup>, S. Uno<sup>168</sup>, S. E. Vahsen<sup>169</sup>, G. Varner<sup>170</sup>, D. Wang<sup>171</sup>, E. Wang<sup>172</sup>, M.-Z. Wang<sup>173</sup>, S. Watanuki<sup>174</sup>, O. Werbycka<sup>175</sup>, E. Won<sup>176</sup>, B. D. Yabsley<sup>177</sup>, W. Yan<sup>178</sup>, J. H. Yin<sup>179</sup>, C. Z. Yuan<sup>180</sup>, L. Yuan<sup>181</sup>, Y. Yusa<sup>182</sup>, Z. P. Zhang<sup>183</sup>, V. Zhilich<sup>184</sup>, and V. Zhukova<sup>185</sup>

(The Belle Collaboration)

We report a study of the hadronic transitions  $\chi_{bJ}(2P) \rightarrow \omega\Upsilon(1S)$ , with  $\omega \rightarrow \pi^+\pi^-\pi^0$ , using  $28.2 \times 10^6 \Upsilon(3S)$  mesons recorded by the Belle detector. We present the first evidence for the near-threshold transition  $\chi_{b0}(2P) \rightarrow \omega\Upsilon(1S)$ , the analog of the charm sector decay  $\chi_{c1}(3872) \rightarrow \omega J/\psi$ , with a branching fraction of  $\mathcal{B}(\chi_{b0}(2P) \rightarrow \omega\Upsilon(1S)) = (0.55 \pm 0.19 \pm 0.07)\%$ . We also obtain branching fractions of  $\mathcal{B}(\chi_{b1}(2P) \rightarrow \omega\Upsilon(1S)) = (2.39^{+0.20}_{-0.19} \pm 0.24)\%$  and  $\mathcal{B}(\chi_{b2}(2P) \rightarrow \omega\Upsilon(1S)) = (0.47^{+0.13}_{-0.12} \pm 0.06)\%$ , confirming the measurement of the  $\omega$  transitions of the  $J = 1, 2 P$ -wave states. The ratio for the  $J = 2$  to  $J = 1$  transitions is also measured and found to differ by 3.3 standard deviations from the expected value in the QCD multipole expansion.

Recently, the hadronic transitions among heavy quarkonium ( $Q\bar{Q}$ , where  $Q = c, b$ ) states have been the focus of detailed study [1–11]. Of such transitions, those occurring near kinematic thresholds for the decay constitute a unique laboratory in which one can study the emission and hadronization of low-momentum gluons [12]. The observation of the near-threshold transition  $\chi_{c1}(3872) \rightarrow \omega J/\psi$  by Belle [13], subsequently confirmed by BaBar [3], BESIII [10], and LHCb [11], is of particular interest. Although it is a narrow state ( $\Gamma_{\chi_{c1}(3872)} = 1.19 \pm 0.21$  MeV [14]) that lies nearly 8 MeV below the nominal kinematic threshold for production of an  $\omega$  and  $J/\psi$  meson, the observed branching fraction of  $(1.9 \pm 0.5)\%$  [11] is nearly as large as that of the discovery channel  $\chi_{c1}(3872) \rightarrow \pi^+\pi^-J/\psi$  [15]. In the bottomonium ( $b\bar{b}$ ) sector, the analogous  $\omega\Upsilon(1S)$  final-state threshold lies between the  $J = 1$  and  $J = 0$  states of the

$\chi_{bJ}(2P)$  triplet, with the latter lying about 10.5 MeV below the nominal threshold.

In 2004, CLEO reported the first observation of the transitions  $\chi_{bJ}(2P) \rightarrow \omega\Upsilon(1S)$  produced in radiative decays of  $(5.81 \pm 0.12) \times 10^6 \Upsilon(3S)$  mesons [16]. The branching fractions of the  $J = 1$  and  $J = 2$  states were measured to be on the order of 1%. To date, no confirmation of the CLEO measurement has been made. Although no indication of a  $J = 0$  signal was seen by CLEO, Monte Carlo (MC) simulation of  $\chi_{b0}(2P)$  transitions to an  $S$ -wave  $\omega\Upsilon(1S)$  indicates that the decay may be observed, though in such transitions the  $\omega$  lineshape is distorted due to the presence of the nearby kinematic threshold. In the charmonium ( $c\bar{c}$ ) sector, BaBar has reported a similar distortion in the lineshape of the  $\omega$  mass for  $\chi_{c1}(3872) \rightarrow \omega J/\psi$  events [3].

In this Letter, we report the first evidence of the

near-threshold transition  $\chi_{b0}(2P) \rightarrow \omega\Upsilon(1S)$  with significance in excess of 3.2 standard deviations, and confirm CLEO's measurement of the corresponding transitions of the  $J = 1$  and  $J = 2$  states. The  $\chi_{bJ}(2P)$  are produced in radiative transitions of the  $\Upsilon(3S)$  at the Belle experiment. The  $\Upsilon(1S)$  is reconstructed in decays to a pair of high-momentum leptons ( $e, \mu$ ), while the  $\omega$  is reconstructed in its decay to  $\pi^+\pi^-\pi^0$ , with  $\pi^0 \rightarrow \gamma\gamma$ . As a normalization sample, we reconstruct the decay  $\Upsilon(3S) \rightarrow \pi^+\pi^-\Upsilon(1S)$  in the final state  $\pi^+\pi^-\ell^+\ell^-$ , which has a branching fraction of  $(2.1 \pm 0.3) \times 10^{-3}$  [14].

The cascade branching ratios,

$$r_{J/1} = \frac{\mathcal{B}(\Upsilon(3S) \rightarrow \gamma\chi_{bJ}(2P) \rightarrow \gamma\omega\Upsilon(1S))}{\mathcal{B}(\Upsilon(3S) \rightarrow \gamma\chi_{b1}(2P) \rightarrow \gamma\omega\Upsilon(1S))}, \quad (1)$$

are also measured and compared with the expectation from the multipole expansion model of quantum chromodynamics (QCDME) [17], which we calculate using the current world averages of bottomonium state masses (or mass differences, where more precisely measured) and branching fractions [14].

We analyze data samples corresponding to an integrated luminosity of  $2.9 \text{ fb}^{-1}$  and  $513.0 \text{ fb}^{-1}$  recorded near the  $\Upsilon(3S)$  and  $\Upsilon(4S)$  resonances, respectively, by the Belle detector [18] at the KEKB asymmetric-energy  $e^+e^-$  collider [19, 20]. We also study a sample, referred to as the off-resonance sample, collected about 60 MeV below the  $\Upsilon(4S)$  resonance, totalling  $56.0 \text{ fb}^{-1}$ . The number of  $\Upsilon(3S)$  in the combined dataset is determined from a reconstruction of  $\Upsilon(3S) \rightarrow \pi^+\pi^-\Upsilon(1S)[\ell^+\ell^-]$  to be  $(28.2 \pm 0.9) \times 10^6$ . Decays of  $\Upsilon(3S)$  mesons in data accumulated above the  $\Upsilon(3S)$  resonance are assumed to come from initial state radiation (ISR) by the  $e^+e^-$  pair. No attempt has been made to reconstruct the ISR photons, which typically emerge at small angles to the beampipe [21].

The Belle detector, described in detail elsewhere [18, 22], is a large-solid-angle magnetic spectrometer that consists of a silicon vertex detector (SVD), a 50-layer central drift chamber (CDC), an array of aerogel threshold Cherenkov counters (ACC), a barrel-like arrangement of time-of-flight scintillation counters, and an electromagnetic calorimeter (ECL) composed of CsI(Tl) crystals located inside a superconducting solenoid coil that provides a 1.5 T magnetic field. The ECL is divided into three regions spanning the polar angle  $\theta$ . The  $z$  axis is taken to be the direction opposite the  $e^+$  beam. The ECL backward endcap, barrel, and forward endcap, cover ranges  $\cos\theta \in [-0.91, -0.65]$ ,  $[-0.63, 0.85]$ , and  $[0.85, 0.98]$ , respectively. An iron flux-return located outside of the coil is instrumented with resistive plate counters to detect  $K_L^0$  mesons and muons (KLM). The data collected for this analysis used an inner detector system with a 1.5 cm beampipe, a 4-layer SVD, and a small-inner-cell CDC.

A set of event selection criteria are devised to optimize the retention of signal events while suppressing

backgrounds from misreconstructed  $\pi^0$  decays, resonant  $b\bar{b}$  decays, and nonresonant (continuum) production of other quark and lepton species. For all optimizations, we employ the figure of merit  $S/\sqrt{S+B}$ , where  $S$  and  $B$  denote the number of signal and background events, respectively. To study these criteria and their associated reconstruction efficiencies, MC simulated events are produced. MC samples containing an admixture of signal  $\chi_{bJ}(2P) \rightarrow \omega\Upsilon(1S)$  and other  $b\bar{b}$  events are prepared assuming the CLEO-measured branching fractions [14, 16]. As no measurement of the  $J = 0$  signal transition exists, it is conservatively taken to be small and equivalent to the  $J = 2$  branching fraction. MC events are generated with the EVTGEN [23] package. Radiative transitions among  $b\bar{b}$  states are assumed to be E1 (i.e. electric dipole) transitions and have been generated according to their helicity amplitudes [24]. Di-pion transitions among the  $\Upsilon(3S)$ ,  $\Upsilon(2S)$ , and  $\Upsilon(1S)$  states are modeled according to the matrix elements reported in Ref. [25]. All other hadronic transitions among  $b\bar{b}$  states are modeled with phase space. Final state radiation effects are modeled by PHOTOS [26]. The Belle detector response is simulated with GEANT3 [27]. The time-varying detector performance and accelerator conditions are taken into account in the simulation.

Reconstructed charged particles are required to originate within 2.0 cm of the interaction point (IP) along the  $z$  axis and within 0.5 cm in the transverse plane. Tracks whose momentum exceeds 4 GeV [28] measured in the center-of-mass (c.m.) frame are preliminarily identified as leptons, and pairs of such tracks are combined to form  $\Upsilon(1S)$  candidates if their invariant mass lies within the range  $M(\ell\ell) \in [9.0, 9.8] \text{ GeV}$ .

A likelihood  $\mathcal{L}_i$  ( $i = \mu, \pi, K$ ) is ascribed to each track based on its signature in the KLM and its agreement with an extrapolation of the track from the CDC. The muon identification likelihood ratio is defined as  $\mathcal{R}_\mu = \mathcal{L}_\mu / (\mathcal{L}_\mu + \mathcal{L}_\pi + \mathcal{L}_K)$  [29]. A similar electron identification likelihood ratio is defined as  $\mathcal{R}_e = \prod_{i=1}^n \mathcal{L}_e^i / \left( \prod_{i=1}^n \mathcal{L}_e^i + \prod_{i=1}^n \mathcal{L}_e^i \right)$ , where  $\mathcal{L}_e^i$  ( $\mathcal{L}_e^i$ ) are the likelihoods associated with  $i$ -th measurements from the CDC, ECL, and ACC, with the assumption that the track is (not) an electron [30]. Both lepton candidates are identified as muons if  $\mathcal{R}_\mu > \mathcal{R}_e$  for either of them; otherwise, they are considered as electrons.

QED continuum processes of the form  $e^+e^- \rightarrow q\bar{q}$ , where  $q = u, d, s, c$ , may mimic our signal. Due to the relatively small production cross section of our signal in the  $\Upsilon(4S)$  dataset, the signal purity is far lower than that of the on-resonance  $\Upsilon(3S)$  dataset. To suppress the higher backgrounds present in  $\Upsilon(4S)$  data, the flavor of  $\Upsilon(1S) \rightarrow \ell^+\ell^-$  is positively reconstructed by requiring that both leptons satisfy  $\mathcal{R}_e > 0.2$  or  $\mathcal{R}_\mu > 0.2$ . The identification efficiency for a muon (electron) pair passing the likelihood ratio criterion is approximately

92%. Moreover, the lepton momenta must satisfy  $p_{\text{c.m.}} < 5.25$  GeV, to avoid a peak from low multiplicity QED processes near  $M(\Upsilon(4S))/2 \simeq 5.29$  GeV.

Due to the limited phase space to produce a pair of charged kaons in conjunction with a neutral pion in events with an  $\Upsilon(1S)$  candidate, all low-momentum tracks in the c.m. frame, satisfying  $p_{\text{c.m.}} < 0.43$  GeV, are treated as pion candidates. Contamination from photon conversion to an  $e^+e^-$  pair in detector material are suppressed by requiring that the cosine of the opening angle between oppositely charged pion candidates be less than 0.95. To reject events with misreconstructed tracks, events with multiple pairs of oppositely charged pions are rejected.

Photons are reconstructed from isolated clusters in the ECL that are not matched with a charged track projected from the CDC. To reject hadronic showers, the ratio of energy deposited in a  $3 \times 3$  and  $5 \times 5$  array of crystals centered on the most energetic one is required to exceed 90%. Clusters with an electromagnetic shower width exceeding 6.0 cm are also rejected. To suppress beam-related backgrounds, photons are required to have an energy greater than 50, 100, and 150 MeV in the barrel, backward and forward endcaps, respectively.

Neutral pion candidates are formed from pairs of photons that satisfy  $M(\gamma\gamma) \in [0.11, 0.15]$  GeV, which is approximately 90% efficient. To reject combinatorial background from misreconstructed  $\pi^0$  candidates, we require that  $p_{\text{c.m.}}^{\pi^0} \in [0.08, 0.43]$  GeV. A kinematic fit is performed to constrain the invariant mass of each candidate to the current world average  $\pi^0$  mass [14], and the best-candidate  $\pi^0$  is selected according the smallest mass-constrained fit  $\chi^2$ . Studies in simulation indicate that the best-candidate selection rejects 45% of the background from misreconstructed  $\pi^0$  at a cost of 14% of the signal. The  $\omega$  candidate is reconstructed as the combination of the  $\pi^0$  and the  $\pi^+\pi^-$  pair; those satisfying the reconstructed  $\omega$  mass  $M_\omega \in [0.71, 0.83]$  GeV are retained for further analysis.

Backgrounds from resonant di-pion bottomonium transitions may mimic our final state  $\pi^+\pi^-\pi^0\ell^+\ell^-$ . The largest source of contamination arises from decay chains containing  $\Upsilon(2S) \rightarrow \pi^+\pi^-\Upsilon(1S)$ , which may be produced through feed-down transitions ( $\pi^+\pi^-$ ,  $\pi^0\pi^0$ , or  $\gamma\gamma$  via  $\chi_{bJ}(2P)$ ) of the  $\Upsilon(3S)$  or directly via ISR. In the  $\Upsilon(4S)$  dataset, additional contamination arises from transitions of the form  $\Upsilon(4S) \rightarrow \pi^+\pi^-\Upsilon(2S)$ , where the  $\Upsilon(2S)$  decays to the  $\Upsilon(1S)$  through similar feed-down transitions. To suppress such events, we develop a veto using the shifted mass difference

$$\Delta M_{\pi\pi} = M(\pi^+\pi^-\ell^+\ell^-) - M(\ell^+\ell^-) + m(\Upsilon(1S)), \quad (2)$$

where the broad resolution of the di-lepton invariant mass is removed by subtracting the reconstructed mass of the leptons and adding back the current world average  $\Upsilon(1S)$

mass [14]. Di-pion transitions between  $b\bar{b}$  states give rise to narrow peaks in the  $\Delta M_{\pi\pi}$  distribution with a resolution of approximately 2 MeV.

Background from  $\Upsilon(3S) \rightarrow \pi^+\pi^-\Upsilon(2S)$  and  $\Upsilon(3S) \rightarrow \pi^+\pi^-\Upsilon(1S)$  events are rejected at no cost in signal efficiency by  $\Delta M_{\pi\pi} > 9.83$  GeV and  $\Delta M_{\pi\pi} < 10.13$  GeV, respectively. A single veto is developed to suppress contamination from  $\Upsilon(2S) \rightarrow \pi^+\pi^-\Upsilon(1S)$  and  $\Upsilon(4S) \rightarrow \pi^+\pi^-\Upsilon(2S)$ , which have nearly overlapping signatures in  $\Delta M_{\pi\pi}$  as a result of the similar mass splittings between the  $n = 2, 4$  and  $n = 1, 2$   $\Upsilon(nS)$  states. A figure of merit optimization yields  $\Delta M_{\pi\pi} \notin (10.017, 10.290)$  GeV for the  $\Upsilon(3S)$  and off-resonance datasets and  $\Delta M_{\pi\pi} \notin (10.014, 10.030)$  GeV for the  $\Upsilon(4S)$  dataset. These requirements reject 92% of resonant  $b\bar{b}$  events at a cost not exceeding 12% of the signal. Table I summarizes the selection efficiency in each channel.

To determine the yield of reconstructed  $\chi_{bJ}(2P)$  signal candidates, we define the shifted mass difference  $\Delta M_\chi$  as  $\Delta M_{\pi\pi}$  (Eq. 2), as

$$\Delta M_\chi = M(\pi^+\pi^-\pi^0\ell^+\ell^-) - M(\ell^+\ell^-) + m(\Upsilon(1S)), \quad (3)$$

where  $M(\pi^+\pi^-\pi^0\ell^+\ell^-)$  is the invariant mass of the  $\chi_{bJ}$  final state. The distribution of signal events is narrowly peaked at the corresponding  $\chi_{bJ}$  masses, with a corresponding resolution of 4.5 – 5.0 MeV, depending on the transition. Signal yields are extracted from a simultaneous extended maximum-likelihood fit to the unbinned  $\Delta M_\chi$  and  $M_\omega$  distributions. The projections of this fit are illustrated in Fig. 1, and the extracted signal yields are summarized in Table I. The  $\chi_{bJ}(2P)$  signal peaks are modeled with a double-sided Crystal Ball function (DSCB) [31], which consists of a Gaussian core that is augmented on either side by power-law tails. The distorted  $M_\omega$  lineshape of the  $J = 0$  transition is parameterized by the product of a DSCB and a sigmoid.

TABLE I. Selection efficiencies, obtained from large samples of simulation, as well as extracted signal yields in data and the associated significances, including systematic uncertainties, expressed in terms of standard deviations ( $\sigma$ ).

$\chi_{bJ}(2P)$	Efficiency (%)	Signal Yield	Significance
$J = 0$	$8.13 \pm 0.02$	$32 \pm 11$	$3.2\sigma$
$J = 1$	$8.35 \pm 0.02$	$304_{-24}^{+26}$	$16.5\sigma$
$J = 2$	$8.36 \pm 0.02$	$62_{-16}^{+17}$	$4.1\sigma$

As the  $\chi_{bJ}(2P)$  are well established resonances, there is no look-elsewhere effect [32]; therefore, it is sufficient to calculate the local significance at fixed mass while leaving the multiplicative resolution calibrations and signal yields free. We verify the applicability of Wilks' theorem with a series of MC pseudoexperiments for each signal using the methodology described in Ref. [33]. The statistical significance, including systematic uncertainties, is

calculated by convolving the profile likelihood [34] with a Gaussian distribution of width equal to the systematic uncertainty of each signal hypothesis. The results are summarized in Table I. The  $J = 0$  peak has a significance of  $3.2\sigma$ : this is the first evidence for the near-threshold

transition  $\chi_{b0}(2P) \rightarrow \omega\Upsilon(1S)$ .

We attribute any  $\chi_{bJ}(2P)$  in  $\Upsilon(4S)$  data solely to radiative decays of ISR produced  $\Upsilon(3S)$  mesons, as transitions of the form  $\Upsilon(4S) \rightarrow X + \chi_{bJ}(2P)$  have not been

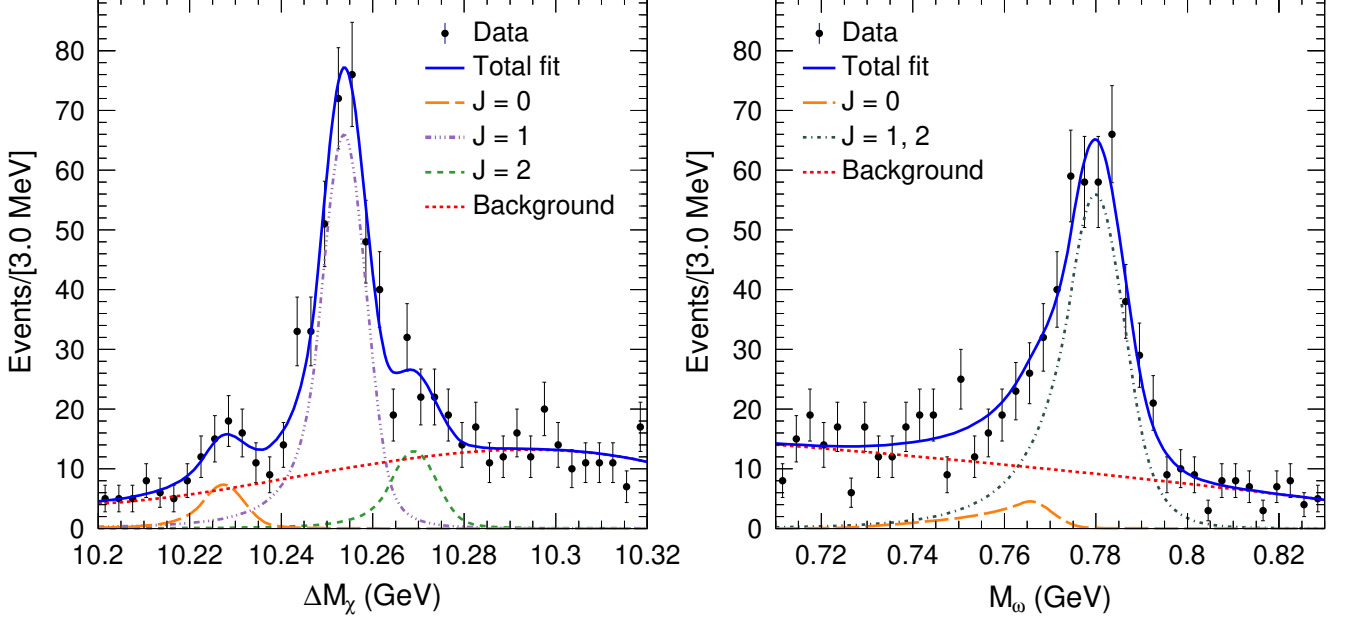


FIG. 1. Fit to the  $\Delta M_\chi$  (left) and  $M_\omega$  (right) distributions for  $\chi_{bJ}(2P) \rightarrow \omega\Upsilon(1S)$  candidates reconstructed in data. The solid blue curves show the total fit and the dotted red curves indicate the background. In both panels, the long dashed orange curves are the  $J = 0$  signal. In the left panel, the dash-dotted violet curve is the  $J = 1$  signal, and the dashed green curve is the  $J = 2$  signal. In the right panel, the dash-dotted gray curve shows the combined  $J = 1$  and 2 signal.

seen [14]. Branching fractions for the three  $\omega$  transitions are calculated from the relevant signal yield  $N_J$  and reconstruction efficiency  $\epsilon_J$  as

$$\mathcal{B}(\chi_{bJ}(2P) \rightarrow \omega\Upsilon(1S)) = \frac{N_J}{\epsilon_J N_{\Upsilon(3S)} \prod \mathcal{B}_i}, \quad (4)$$

where  $\prod \mathcal{B}_i$  is the product of the  $\Upsilon(3S) \rightarrow \gamma\chi_{bJ}(2P)$ ,  $\Upsilon(1S) \rightarrow \ell^+\ell^-$ ,  $\omega \rightarrow \pi^+\pi^-\pi^0$ , and  $\pi^0 \rightarrow \gamma\gamma$  branching fractions. The number of  $\Upsilon(3S)$  events  $N_{\Upsilon(3S)}$  is determined from a concurrent reconstruction of  $\Upsilon(3S) \rightarrow \pi^+\pi^-\Upsilon(1S)[\ell^+\ell^-]$  events. Leptons and pions are reconstructed and combined to form di-pion and  $\Upsilon(1S)$  candidates with selection criteria identical to those used to reconstruct  $\chi_{bJ}(2P) \rightarrow \omega\Upsilon(1S)$  events, with the caveat that the pion momentum is relaxed to  $p_{c.m.} < 0.7$  GeV. Additionally, the four charged tracks combine to form a shifted invariant mass  $\Delta M_{\pi\pi}$  lying in the signal range of [10.28, 10.42] GeV. The resulting reconstruction efficiency ( $\epsilon_{\pi\pi\Upsilon}$ ) is  $(41.37 \pm 0.03)\%$ . The  $\pi\pi\Upsilon(1S)$  yield  $N_{\pi\pi\Upsilon}$  is extracted from an extended maximum-likelihood fit to the unbinned data shown in Fig. 2. The signal is parameterized with a DSCB and the background with a

linear function. A signal yield of  $24756^{+234}_{-233} \pm 99$  events is obtained, where the first uncertainty is statistical and the second is systematic. The corresponding number of  $\Upsilon(3S)$  events is calculated as:

$$N_{\Upsilon(3S)} = \frac{N_{\pi\pi\Upsilon}}{\epsilon_{\pi\pi\Upsilon} \mathcal{B}(\Upsilon(3S) \rightarrow \pi^+\pi^-\Upsilon(1S)[\ell^+\ell^-])}, \quad (5)$$

yielding  $(28.2 \pm 0.3 \pm 0.9) \times 10^6$  events, where the statistical and systematic uncertainties are quoted, respectively. The systematic uncertainty is the sum in quadrature of the following sources: tracking (1.3%), lepton identification (0.4%), fit procedure (0.4%), input branching fractions (3.1%), and the efficiency (0.1%).

In the combination of Eqs. 4 and 5, the  $\Upsilon(1S) \rightarrow \ell^+\ell^-$  branching fraction cancels. Using the present world averages [14], we obtain

$$\begin{aligned} \mathcal{B}(\chi_{b0}(2P) \rightarrow \omega\Upsilon(1S)) &= (0.55 \pm 0.19 \pm 0.07)\% \\ \mathcal{B}(\chi_{b1}(2P) \rightarrow \omega\Upsilon(1S)) &= (2.39^{+0.20}_{-0.19} \pm 0.24)\% \\ \mathcal{B}(\chi_{b2}(2P) \rightarrow \omega\Upsilon(1S)) &= (0.47^{+0.13}_{-0.12} \pm 0.06)\% \end{aligned} \quad (6)$$

where the first uncertainty is statistical and the second

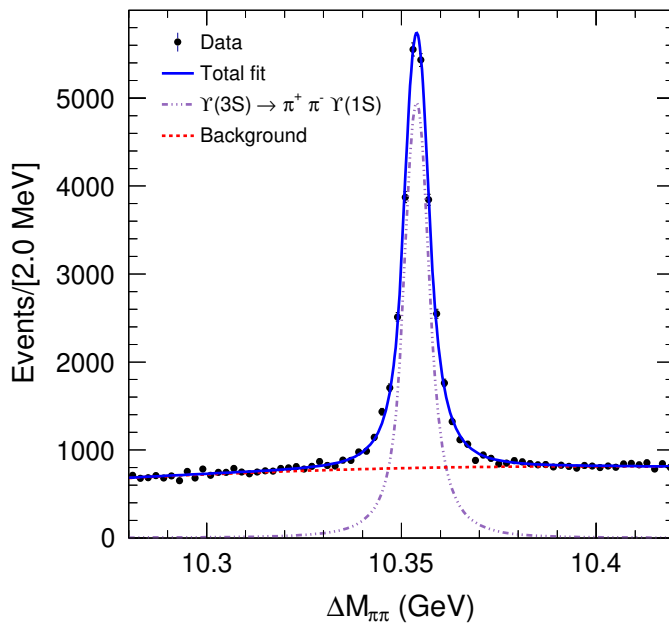


FIG. 2. Fit to the distribution of  $\Delta M_{\pi\pi}$  in data for candidate  $\Upsilon(3S) \rightarrow \pi^+\pi^-\Upsilon(1S)$  events. The total fit is shown by the solid blue curve, the background contribution by the dotted red curve, and the signal contribution by the dash-dotted violet curve. The overlaid signal shape.

is systematic. The  $J = 1, 2$  measurements are consistent with the CLEO results [16] at less than  $2\sigma$ . It is worth noting that the  $J = 0$  and  $J = 2$  rates are consistent with one another, despite the broader natural width of the  $J = 0$  state and the limited phase space for the transition.

Save for the  $J = 1$  measurement, the statistical uncertainty dominates. In obtaining the quoted systematic uncertainties, individual uncertainties have been assigned for  $\pi^0$  reconstruction (0.9%), the number of  $\Upsilon(3S)$  (1.0%), and MC statistics (0.2%). In the normalization procedure, systematic uncertainties due to data-MC differences in track finding, lepton identification, and the  $\Upsilon(1S) \rightarrow \ell^+\ell^-$  branching fraction cancel. The uncertainty on each signal yield due to the signal extraction procedure is estimated by repeating fits to data changing fit window, background parameterization, values of shape parameters fixed from signal MC events. The systematic uncertainty from each source is summed in quadrature to estimate the uncertainty assigned to signal extraction ( $+8.0\%$ ,  $+1.8\%$ , and  $+3.1\%$  for the  $J = 0, 1$ , and  $2$  states, respectively). The relative uncertainties on the branching fractions for  $\Upsilon(3S) \rightarrow \gamma\chi_{bJ}(2P)$ ,  $\Upsilon(3S) \rightarrow \pi^+\pi^-\Upsilon(1S)$ ,  $\omega \rightarrow \pi^+\pi^-\pi^0$ , and  $\pi^0 \rightarrow \gamma\gamma$  constitute the largest source of systematic uncertainty in the analysis (10.4%, 9.7%, and 12.4% for the  $J = 0, 1$ , and  $2$  states, respectively). These uncertainties are combined in quadrature to obtain the total systematic uncertainty on each measurement.

In the nonrelativistic limit of QCDME, the spin depen-

dence of the decay amplitude  $\Gamma(\chi_{bJ}(2P) \rightarrow \omega\Upsilon(1S))$  factorizes. In the ratio  $r_{2/1}$ , defined in Eq. 1, the spin of the heavy quark decouples and the ratio of the  $\omega\Upsilon(1S)$  decay amplitudes may be approximated as the ratio of the  $S$ -wave phase space factors  $\Delta_J = M_{\chi_{bJ}(2P)} - M_{\Upsilon(1S)} - M_\omega$ . Following the methodology presented in Ref. [17], we calculate this ratio using current world averages [14] as  $r_{2/1}^{\text{QCDME}} = 0.77 \pm 0.16$ , a  $3.3\sigma$  shift from the previously reported value of  $1.3 \pm 0.3$  [17].

To measure  $r_{J/1}$ , we reparameterize the fit in terms of the signal yield ratios  $P_{J/1} = N_J/N_1$ , for  $J = 0, 2$ . Correcting the results for the relevant efficiencies as  $r_{J/1} = P_{J/1}(\epsilon_1/\epsilon_J)$ , we obtain  $r_{0/1} = 0.107^{+0.038}_{-0.036} \pm 0.009$  and  $r_{2/1} = 0.205^{+0.062+0.007}_{-0.056-0.010}$ . In each ratio  $r_{J/1}$ , only the systematic uncertainties assigned for signal extraction and the selection efficiency (on each yield) contribute. This  $r_{2/1}$  measurement differs from the expectation from QCDME [17] by  $3.3\sigma$ . It should be noted that this test of QCDME is limited not by the statistics of our sample, but by the measured values of radiative  $b\bar{b}$  branching fractions used in the calculation of  $r_{2/1}^{\text{QCDME}}$ .

In summary, we have used the combined  $\Upsilon(3S)$  and  $\Upsilon(4S)$  data samples collected by the Belle detector to obtain the first evidence for the near-threshold transition  $\chi_{b0}(2P) \rightarrow \omega\Upsilon(1S)$  produced in radiative  $\Upsilon(3S)$  decays with a branching fraction of  $(0.55 \pm 0.19 \pm 0.07)\%$  at a significance of  $3.2\sigma$ . Moreover, we measure the hadronic transitions  $\mathcal{B}(\chi_{b1}(2P) \rightarrow \omega\Upsilon(1S)) = (2.39^{+0.20}_{-0.19} \pm 0.24)\%$  and  $\mathcal{B}(\chi_{b2}(2P) \rightarrow \omega\Upsilon(1S)) = (0.47^{+0.13}_{-0.12} \pm 0.06)\%$ . This constitutes the first confirmation of the  $J = 1$  and  $J = 2$  branching fractions since their discovery [16]. The cascade branching fraction ratios  $r_{J/1}$  are also measured. Comparison of the resulting measurement of  $r_{2/1}$  with the theoretical expectations from QCDME—based on multipole expansions of  $S$ -wave phase space factors—reveals a  $3.3\sigma$  tension.

This work, based on data collected using the Belle detector, which was operated until June 2010, was supported by the Ministry of Education, Culture, Sports, Science, and Technology (MEXT) of Japan, the Japan Society for the Promotion of Science (JSPS), and the Tau-Lepton Physics Research Center of Nagoya University; the Australian Research Council including grants DP210101900, DP210102831, DE220100462, LE210100098, LE230100085; Austrian Federal Ministry of Education, Science and Research and Austrian Science Fund (FWF) No. P 31361-N36; National Key R&D Program of China under Contract No. 2022YFA1601903, National Natural Science Foundation of China and research grants No. 11575017, No. 11761141009, No. 11705209, No. 11975076, No. 12135005, No. 12150004, No. 12161141008, and No. 12175041, and Shandong Provincial Natural Science Foundation Project ZR2022JQ02; the Czech Science Foundation Grant No. 22-18469S; Horizon

2020 ERC Advanced Grant No. 884719 and ERC Starting Grant No. 947006 “InterLeptons” (European Union); the Carl Zeiss Foundation, the Deutsche Forschungsgemeinschaft, the Excellence Cluster Universe, and the VolkswagenStiftung; the Department of Atomic Energy (Project Identification No. RTI 4002), the Department of Science and Technology of India, and the UPES (India) SEED finding programs Nos. UPES/R&D-SEED-INFRA/17052023/01 and UPES/R&D-SOE/20062022/06; the Istituto Nazionale di Fisica Nucleare of Italy; National Research Foundation (NRF) of Korea Grant Nos. 2016R1D1A1B02012900, 2018R1A2B3003643, 2018R1A6A1A06024970, RS2022-00197659, 2019R1I1A3A01058933, 2021R1A6A1A-03043957, 2021R1F1A1060423, 2021R1F1A1064008, 2022R1A2C1003993; Radiation Science Research Institute, Foreign Large-size Research Facility Application Supporting project, the Global Science Experimental Data Hub Center of the Korea Institute of Science and Technology Information and KREONET/GLORIAD; the Polish Ministry of Science and Higher Education and the National Science Center; the Ministry of Science and Higher Education of the Russian Federation and the HSE University Basic Research Program, Moscow; University of Tabuk research grants S-1440-0321, S-0256-1438, and S-0280-1439 (Saudi Arabia); the Slovenian Research Agency Grant Nos. J1-9124 and P1-0135; Ikerbasque, Basque Foundation for Science, and the State Agency for Research of the Spanish Ministry of Science and Innovation through Grant No. PID2022-136510NB-C33 (Spain); the Swiss National Science Foundation; the Ministry of Education and the National Science and Technology Council of Taiwan; and the United States Department of Energy and the National Science Foundation. These acknowledgements are not to be interpreted as an endorsement of any statement made by any of our institutes, funding agencies, governments, or their representatives. We thank the KEKB group for the excellent operation of the accelerator; the KEK cryogenics group for the efficient operation of the solenoid; and the KEK computer group and the Pacific Northwest National Laboratory (PNNL) Environmental Molecular Sciences Laboratory (EMSL) computing group for strong computing support; and the National Institute of Informatics, and Science Information Network 6 (SINET6) for valuable network support. This material is based in part on work supported by the U.S. Department of Energy, Office of Science, Office of Workforce Development for Teachers and Scientists, Office of Science Graduate Student Research (SCGSR) program. The SCGSR program is administered by the Oak Ridge Institute for Science and Education (ORISE) for the DOE. ORISE is managed by ORAU under contract number DE-SC0014664.

- 
- [1] K. F. Chen *et al.* (Belle Collaboration) Phys. Rev. Lett. **100**, 112001 (2008).
  - [2] B. Aubert *et al.* (BaBar Collaboration), Phys. Rev. D **78**, 112002 (2008).
  - [3] P. del Amo Sanchez *et al.* (BaBar Collaboration), Phys. Rev. D **82**, 011101 (2010).
  - [4] J. P. Lees *et al.* (BaBar Collaboration), Phys. Rev. D **84**, 092003 (2011).
  - [5] I. Adachi *et al.* (Belle Collaboration), Phys. Rev. Lett. **108**, 032001 (2012).
  - [6] U. Tamponi *et al.* (Belle Collaboration), Phys. Rev. Lett. **115**, 142001 (2015).
  - [7] E. Guido *et al.* (Belle Collaboration), Phys. Rev. D **96**, 052005 (2017).
  - [8] E. Guido *et al.* (Belle Collaboration), Phys. Rev. Lett. **121**, 062001 (2018).
  - [9] P. Oskin *et al.* (Belle Collaboration), Phys. Rev. D **102**, 092011 (2020).
  - [10] M. Ablikim *et al.* (BESIII Collaboration), Phys. Rev. Lett. **122**, 232002 (2019).
  - [11] R. Aaij *et al.* (LHCb Collaboration), Phys. Rev. D **108**, L011103 (2023).
  - [12] N. Brambilla *et al.*, Eur. Phys. J. C **71**, 1534 (2011).
  - [13] S. K. Choi *et al.* (Belle Collaboration), Phys. Rev. Lett. **94**, 182002 (2005).
  - [14] R. L. Workman *et al.* (Particle Data Group), Prog. Theor. Exp. Phys. **2022**, 083C01 (2022) and 2023 update.
  - [15] S. K. Choi *et al.* (Belle Collaboration), Phys. Rev. Lett. **91**, 262001 (2003).
  - [16] D. Cronin-Hennessy *et al.* (CLEO Collaboration), Phys. Rev. Lett. **92**, 222002 (2004).
  - [17] M. B. Voloshin, Mod. Phys. Lett. A **18**, 1067 (2003).
  - [18] A. Abashian *et al.* (Belle Collaboration), Nucl. Instrum. Methods Phys. Res., Sect. A **479**, 117 (2002).
  - [19] S. Kurokawa and E. Kikutani, Nucl. Instrum. Methods Phys. Res., Sect. A **499**, 1 (2007).
  - [20] T. Abe *et al.*, Prog. Theor. Exp. Phys. **2013**, 1 (2013).
  - [21] M. Benayoun *et al.*, Mod. Phys. Lett. A **14**, 2605 (1999).
  - [22] J. Brodzicka *et al.* (Belle Collaboration), Prog. Theor. Exp. Phys. **2012**, 04D001 (2012).
  - [23] D. J. Lange, Nucl. Instrum. Methods Phys. Res., Sect. A **462**, 152 (2001).
  - [24] M. Jacob and G. C. Wick, Annals Phys. **7**, 404 (1959).
  - [25] A. Cronin-Hennessy *et al.* (CLEO Collaboration), Phys. Rev. D **76**, 072001 (2007).
  - [26] E. Barberio and Z. Was, Comput. Phys. Commun. **79**, 291 (1994).
  - [27] R. Brun, F. Bruyant, M. Maire, A. C. McPherson, and P. Zancarini, CERN-DD-EE-84-1, (1987).
  - [28] We use units in which the speed of light is  $c = 1$ .
  - [29] A. Abashian *et al.*, Nucl. Instrum. Methods Phys. Res., Sect. A **491**, 69 (2002).
  - [30] K. Hanagaki *et al.*, Nucl. Instrum. Methods Phys. Res., Sect. A **485**, 3 (2002).
  - [31] M. Oreglia, PhD Thesis, Stanford University, Phys. Dept. SLAC-R-236 (1980).
  - [32] E. Gross and O. Vitells, Eur. Phys. J. C **70**, 525 (2010).
  - [33] K. Chilikin *et al.* (Belle Collaboration) Phys. Rev. D **90**, 112009 (2014).
  - [34] G. Cowan *et al.* Eur. Phys. J. C **71**, 1554 (2011).